Millikan Oil-Drop Experiment

Aleksandr Beliaev (1010856744)

Sheng (Bob) Dai (1010865342)

October 28, 2025

Abstract

This experiment reproduces Millikan's historic measurement demonstrating that electric charge is quantized. The purpose of this experiment was to determine the charge of an electron by observing the motion of charged oil droplets in a controllable, uniform electric field. For almost 100 droplets to calculate the charge, the terminal velocities of the droplets were measured, during which the droplets moved upward, downward, and remained stationary, and the corresponding voltages were recorded. The measured charges were found to occur in integer multiples of a fundamental value, yielding an experimental estimate of the elementary charge of $e = (1.59 \pm 0.01) \times 10^{-19}$C, based on a median value from both measurement methods. Method 1 determined the charge using the stopping voltage of a stationary droplet, while Method 2 used the velocities of a rising and falling droplet under different electric fields. The primary source of error came from the uncertainty during tracking and voltage fluctuations.

Contents

1 Introduction

In 1897, J.J.Thompson discovered electrons, a subatomic particle whose electric charge is negative one elementary charge [1]. From then on, scientists were dedicated to measuring their charge, but the measurement always came with a huge error, until the creation of the Millikan Oil-Drop Experiment [2].

The Millikan Oil-Drop Experiment is a cornerstone in modern physics because it provided the first direct measurement of the elementary electric charge and demonstrated that electric charge is quantized, which means it exists only in discrete units. The purpose of this experiment was to measure the elementary charge and confirm charge quantization, comparing the result to the accepted value of $e = 1.602 \times 10^{-19}$ C. The experiment measures the charge of oil drops by balancing the gravitational and electric forces on tiny charged oil droplets suspended between two metal plates. By adjusting the applied voltage, an individual droplet can be made to rise, fall, or remain stationary as the electric force acting on its charge balances the gravitational and buoyant forces acting on its mass. The oil droplets are subjected to different forces: a downward gravitational force $G = m_{\text{oil}}g$, an upward buoyancy force $F_b = -m_{\text{air}}g$, an electric force $F_E = qE$ due to the electric field, and a drag force $F_d = 6\pi\eta r v$ if the oil droplet is moving [3].

Table 1: Notation [3]

Notation	Meaning
m_{oil}	Mass of oil droplets
m_{air}	Mass of air that oil droplets occupied
E	Electric field
r	Radius of oil droplets
η	Fluid viscosity of air
v	Speed of oil droplets

Since electrons have the minimum value of a negative charge, the value of a charge can be calculated by measuring multiple oil drops with different charges and then calculating their greatest common divisor (GCD), where the GCD represents the charge of a single electron. Alternatively, a histogram can be used to display charges to see the quantization.

2 Materials and Methods

This experiment aimed to determine the electric charge of an electron by observing the motion of microscopic charged oil droplets suspended between two parallel metal plates that carry large voltages. The apparatus used was a Millikan oil-drop chamber equipped with a light source, a high-voltage power supply, and a digital microscope connected to a CCD camera for real-time tracking. Oil droplets were introduced into the chamber using a manual pump. After pumping oil droplets into the chamber, by adjusting the voltage across the plates, individual droplets could be made to rise, fall, or remain stationary under the competing influences of gravitational, electric, and viscous forces. Measurements of droplet motion and plate voltage were recorded using Millikan software, and these data were analyzed to calculate the charge on each droplet and, through statistical comparison, to determine the fundamental charge of the electron.

2.1 Materials

The apparatus used was the Leybold-Heraeus Oil Drop apparatus (shown in Figure 1)[3]. The apparatus consists of a transparent observation chamber forming a parallel-plate capacitor, a microscope with CCD camera, and a DC power supply used to create and control the charge between the electric plates. A light source illuminates the droplets and an oil atomizer introduces small charged oil particles to the chamber.

Data acquisition was done with Millikan experiment software, which tracks droplet's vertical position every 0.1 (s) and exports the positions as an excel file. Calibration of the camera determined a scale factor of 540 ± 1 px/mm for the left camera and 520 ± 1 px/mm for the right[3]. Only the right apparatus would be used to collect the data analyzed.

The constant values were used as stated in the following page [3].

2.2 Experimental Procedure

The following experimental procedure was completed to record the data [3]. Before the experiment was conducted, the room lights were turned off and door shut to darken the environment as much as possible. The setup was initialized by turning the DC power supply, light and computer. Millikan software was launched. To make droplets most visible, Upper Gain was dragged to its maximum, and lower gain was slowly raised until droplets appeared faint gray on a black back-

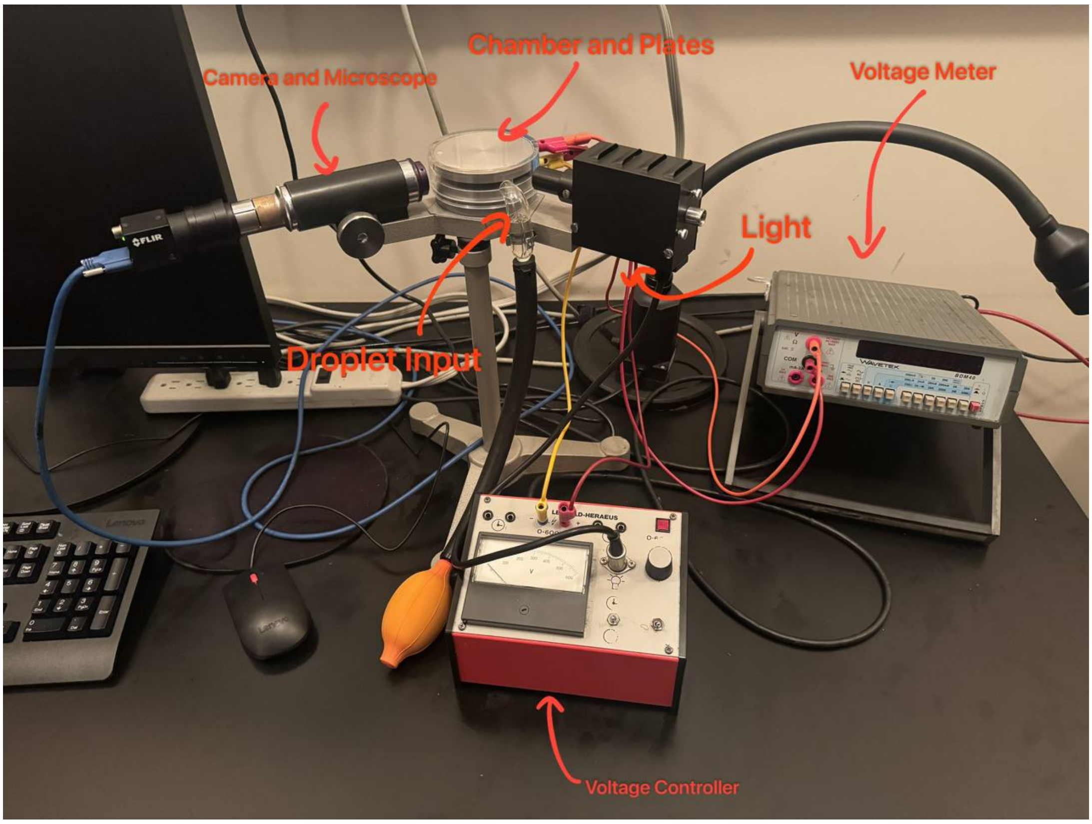

Figure 1: A labeled photo of the lab setup is shown above. An observation chamber with electric plates has a light source and a camera attached to it to observe particle motion.

ground. Microscope focus was also adjusted. After squeezing the bulb 2-3 times with the voltage set high (ranges varied during the experiment), the screen was observed. A properly focused relatively stationary droplet was selected and tracked using the software. The Track Image and Save Data functions were used to record its motion under varying voltages. The voltage would first be raised to let the particle climb at terminal velocity and then set to 0 to observe the terminal falling velocity. The right screen would show a line of motion, which can be used to determine whether the droplet is moving at a constant speed or staying still. Stationary voltage and voltage required to raise the particle were recorded. The tracking done by the Millikan Software would be saved to an excel file.

Table 2: Constant Values

Constant	Notation	Value
Density of oil	ρ_{oil}	875.3 ± 0.4 kg $\cdot$ m^{-3} [4]
Density of air	ρ_{air}	1.204 ± 0.001 kg $\cdot$ m^{-3} [5]
Acceleration due to gravity	g	9.80 ± 0.007 m $\cdot$ s^{-2} [5]
Dynamic viscosity of air at 1 atm	η	$(1.85 \pm 0.06) \times 10^{-5}$ Pa $\cdot$ s [6]
The separation of the parallel plates	d	6.0 ± 0.05 mm [3]

Note. Uncertainties for ρ_{oil}, ρ_{air}, and η were estimated based on the relative errors from their respective sources. The uncertainty in g was obtained from the difference between the constant used and the standard reference value. The uncertainty in d was determined according to the rule of rounding.

The process would repeat for 30 times for the authors. Later, the droplet charge would be computed using two approaches described in the Analysis section.

3 Data and Analysis

3.1 Raw Data and Velocity Calculation

Each droplet's motion was recorded as a position pixel vs time, as described in Experimental Procedure. A CSV file with the first column for time and columns - 2 for each particle, 1 tracking movement down, and 1 tracking movement up - was constructed. The CSV file holds paths of 97 particles, collected by 3 teams. Data collected by authors are from the 67th until the 97th columns. The CSV file, voltage data and the analysis pipeline can be found in the GitHub repo below [7].

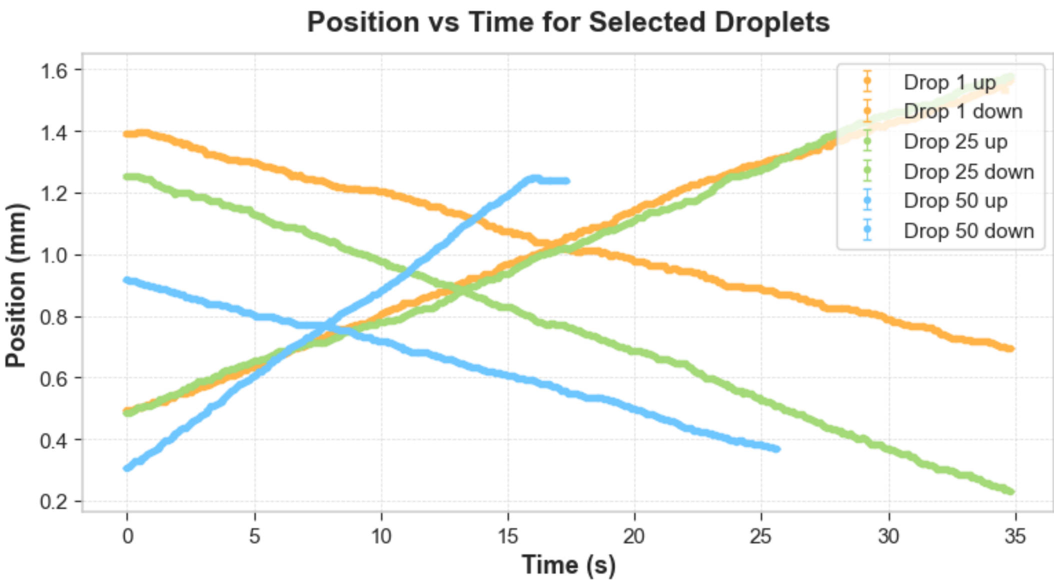

Figure 2: Position vs. time for representative droplets. Each line fitted by least-squares to determine terminal velocity; error bars are smaller than marker size. A relatively constant change of position is clearly seen in the graph.

Before analysis, the "stuck" points were removed using a threshold of 10 consecutive identical readings. Since moving up on the screen was moving down between the plates, according to the calibration, on the right machine [3]:

$$y_{\mathrm{mm}} = \frac{(1024 \times y_{\mathrm{pixels}})}{520}. \tag{1}$$

Uncertainty was propagated, assuming an uncertainty of 0.5px for tracking noise, 1px of calibration of the conversion, and assuming a 0.05s time uncertainty [3].

The terminal velocity of each droplet was obtained by performing a least-squares linear regression of its position-time data, where the slope is the velocity.

$$y = vt + b \tag{2}$$

The data was split up into 5 equal segments, for each of which a linear fit was performed separately. Any velocity that deviated by more than two standard deviations from the median was excluded from final average. This was done to insure that the data used for charge calculations contained only the droplet moving at a constant velocity.

Table 3: Regression/Fit Statistics for Selected Droplets.

Droplet	Slope (velocity) [mm/s]	R^2	Reduced χ^2	N points
1u	-0.02041 ± 0.0005	0.9979	3.491	349
1d	0.03152 ± 0.0009	0.9974	5.227	349
25u	-0.03001 ± 0.0005	0.9992	13.933	349
25d	0.03211 ± 0.0007	0.9982	9.005	349
50u	-0.02141 ± 0.0007	0.9970	12.254	257
50d	0.05765 ± 0.0023	0.9973	9.988	174

Negative slopes correspond to upward movement.

The regression results and fit statistics for representative droplets are summarized in Table 3. Average R^2 values exceeded 0.98, confirming that the model accurately described the particle's motion. The reported reduced χ^2 values are artificially large - effectively meaningless at that scale - because the assigned point-to-point uncertainties were very small, however visual inspection (refer to Figure 2) showed no curvature or systemic residuals. The mean fit parameters across all usable droplets and track are listed in Table 4. The overall mean slope magnitude was of order 10^{-2}mm/s, with a relative uncertainty of about 2%, consistent with expectations and test calculations.

Table 4: Average Regression/Fit Statistics for used Droplets.

Mean Slope [mm/s]	Mean R^2	Mean Reduced χ^2	N tracks
0.00439 ± 0.03651	0.9786 ± 0.1263	$(1.19 \pm 13.61) \times 10^2$	131

3.2 Radius Computation and Cunningham Correction

Droplet radius is required for both methods of finding a droplet's charge (refer to section 3.3). The droplet radius depends on the balance of viscous drag and buoyant-corrected gravity. First, continuous flow was assumed and radius was calculated from the measured terminal velocity v_d. Using Stoke's Law:

$$r = \sqrt{\frac{9\,\eta\,v_d}{2\,g\,(\rho_{\text{oil}} - \rho_{\text{air}})}} \tag{3}$$

Since droplets are below a micrometer in size (refer to Figure 3), a Cunningham correction factor is needed to compensate for the finite mean free path of air molecules. The radius is corrected iteratively three times by first computing

$$C_i = 1 + \frac{b_p}{r} \tag{4}$$

Then, radius is then corrected iteratively 3 times as follows

$$r_{i+1} = \sqrt{\frac{9\,\eta\,v_d\,C_i}{2\,g\,(\rho_{\text{oil}} - \rho_{\text{air}})}} \tag{5}$$

C is often between 1.12 to 1.18 (refer to Figure 2) it noticeably affects the estimated radius of a droplet. It is especially important as radius uncertainties are around 1%, where Cunningham's Correction factor increases it up to 9.5%. From Figure 2, it is also noticeable that droplets with a smaller r tend to have larger C and vice versa, as expected.

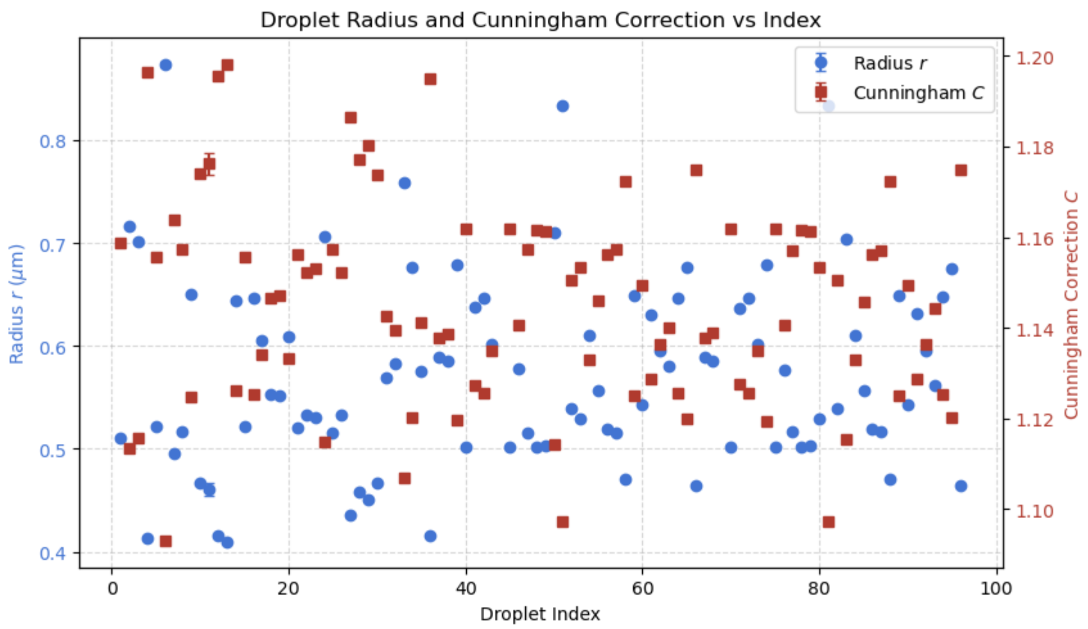

Figure 3: The radius of droplets (blue) and their Cunningham's slip correction factor (red) are displayed. r is between 0.5 and 1 μm, while C is between 1.10 and 1.20. Error bars are invisible outside vertical error bars for one droplet.

Uncertainty in r arises from the uncertainties in viscosity, gravity, densities, and velocity. The uncertainty in r rises slightly with each iteration. Due to the uncertainty exceeding 1% on the 4th iterations, the authors elected to settle for 3 iterations. Propagating in quadrature yields:

$$\left(\frac{\sigma_r}{r}\right)^2 = \frac{1}{4}\left[\left(\frac{\sigma_\eta}{\eta}\right)^2 + \left(\frac{\sigma_{v_d}}{v_d}\right)^2 + \left(\frac{\sigma_g}{g}\right)^2 + \left(\frac{\sigma_{\rho_{\text{oil}}} + \sigma_{\rho_{\text{air}}}}{\rho_{\text{oil}} - \rho_{\text{air}}}\right)^2\right] \tag{6}$$

$$\sigma_C = \sqrt{\left(\frac{\sigma_{b_p}}{r}\right)^2 + \left(\frac{b_p\,\sigma_r}{r^2}\right)^2} \tag{7}$$

3.3 Charge Calculation

There are three states of the droplet observed: stationary, moving up with a constant velocity, and falling with a constant velocity. Using Newton's first law and given $E = \frac{V_{\text{rise}}}{d}$, the equilibrium of forces of each state is listed below [3]:

$$\text{Droplet moving up:} \quad qE = (m_{\text{oil}} - m_{\text{air}})g + 6\pi\eta r v_u \tag{8}$$

$$\text{Droplet moving down:} \quad (m_{\text{oil}} - m_{\text{air}})g = 6\pi\eta r v_d \tag{9}$$

$$\text{Droplet stationary:} \quad (m_{\text{oil}} - m_{\text{air}})g = q\frac{V_{\text{stop}}}{d} \tag{10}$$

Where v_d and v_u are the terminal velocities down and up, respectively, V_{stop} is the voltage between plates, and d is the separation between plates.

3.3.1 Method 1

Method 1 focuses on using the voltage required to keep a droplet stationary and its falling velocity. From the equations above, the droplet's effective weight is given by:

$$W = (m_{\text{oil}} - m_{\text{air}})g = \frac{4}{3}\pi r^3(\rho_{\text{oil}} - \rho_{\text{air}})g. \tag{11}$$

At terminal velocity during free fall, the gravitational and viscous drag forces balance,

$$6\pi\eta r v_d = W. \tag{12}$$

Rearranging gives the droplet radius in terms of the measured falling velocity,

$$r = \sqrt{\frac{9\eta v_d}{2g(\rho_{\text{oil}} - \rho_{\text{air}})}}. \tag{13}$$

When the droplet is held stationary by an electric field $E = V_{\text{stop}}/d$, the electric and gravitational forces balance,

$$qE = W. \tag{14}$$

Substituting the expressions for W and E yields

$$q = \frac{4}{3}\pi r^3(\rho_{\text{oil}} - \rho_{\text{air}})g\frac{d}{V_{\text{stop}}}. \tag{15}$$

Alternatively, combining constants gives the simplified empirical form

$$q = C_1\, v_d^{3/2}\,\frac{V_{\text{stop}}}{d}, \qquad C_1 = \frac{(6\pi\eta)^{3/2}d}{\sqrt{\frac{4}{3}\pi(\rho_{\text{oil}} - \rho_{\text{air}})g}}. \tag{16}$$

C_1 is found by computing the radius as described in section 3.2. Since d is a constant, the charge q can be computed by using the experimentally determined V_{stop} and v_d.

3.3.2 Method 2

When the droplet moves upward at a constant speed v_u under an applied voltage V_{rise}, the electric, drag, and gravitational forces satisfy

$$qE = (m_{\text{oil}} - m_{\text{air}})g + 6\pi\eta r v_u, \tag{17}$$

where $E = V_{\text{rise}}/d$.

During downward motion at terminal velocity v_d with the field off,

$$(m_{\text{oil}} - m_{\text{air}})g = 6\pi\eta r v_d. \tag{18}$$

Eliminating r and combining the two equations gives

$$q = \frac{(m_{\text{oil}} - m_{\text{air}})g(v_d + v_u)}{Ev_d} = \frac{4}{3}\pi r^3(\rho_{\text{oil}} - \rho_{\text{air}})g\frac{(v_d + v_u)d}{v_d V_{\text{rise}}}. \tag{19}$$

Since g, d, ρ_{oil}, ρ_{air} are constants and we can determine r (refer to section 3.2), charge can be computed using experimentally determined v_d, v_u, and V_{rise}.

3.3.3 Particle Charge Computation Results

Using the two methods derived above, charges for every droplet with a continuous velocity were determined (refer to Figures 4 and 5).

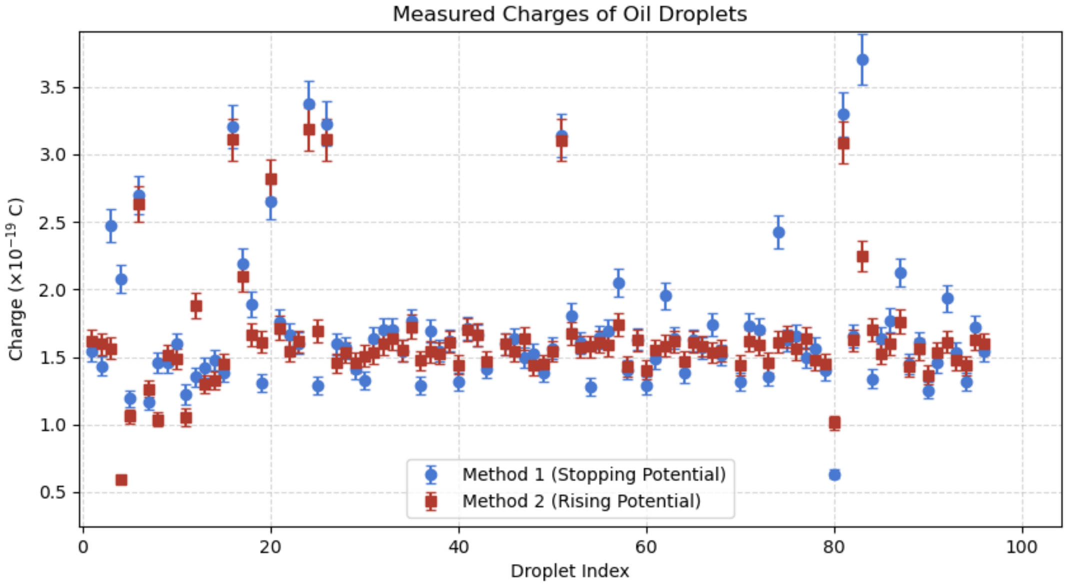

Figure 4: Final computed charges and their associated uncertainties are shown with charges on the y-axis. Method 2 is in red, and method 1 is in blue. Visually, Method 1 seems to have higher estimates compared to Method 2.

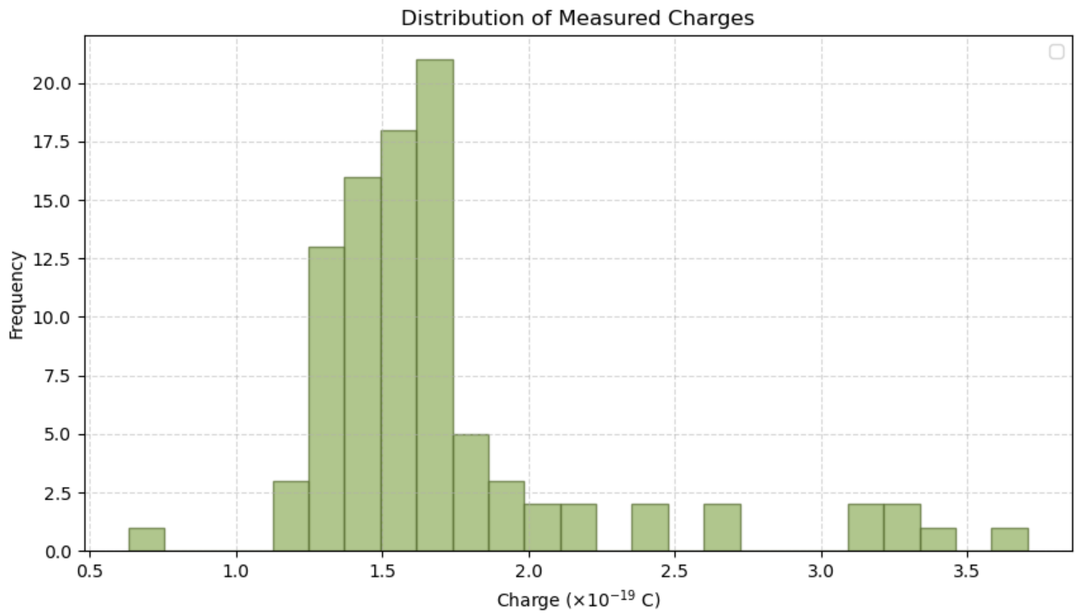

Figure 5: A distribution of charge differences is displayed. The grouping around 1.6 agrees with the estimated charge values and supports quantization of electric charge.

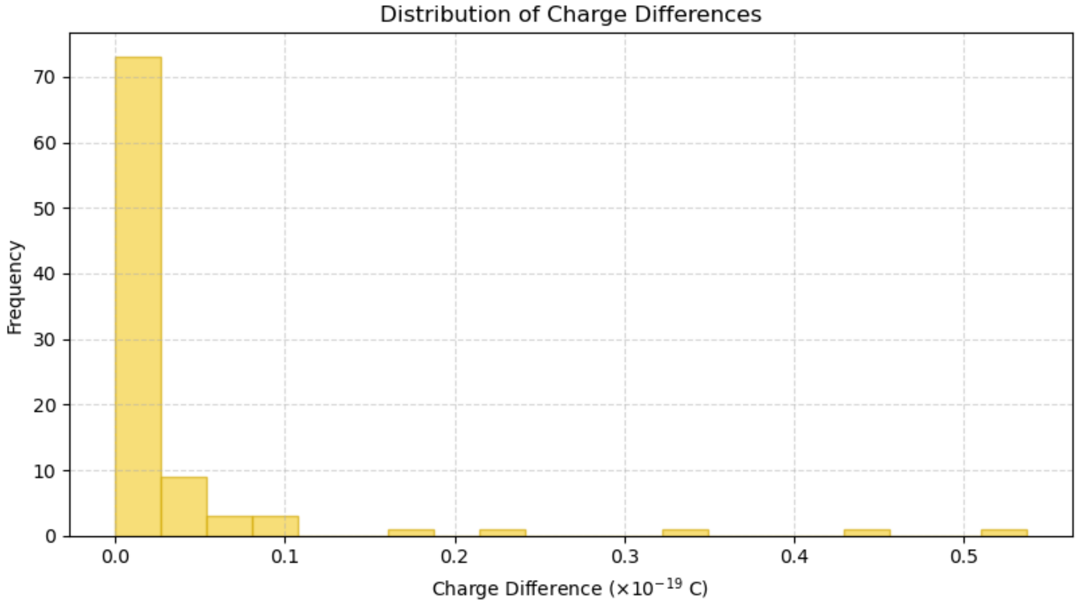

Figure 6: Comparison of charge differences between droplets. The narrow clustering confirms charge quantization within experimental uncertainty.

For both methods, uncertainties were propagated as follows: For Method 1:

$$\left(\frac{\sigma_{q_1}}{q_1}\right)^2 = (3\,\frac{\sigma_r}{r})^2 + \left(\frac{\sigma_d}{d}\right)^2 + \left(\frac{\sigma_g}{g}\right)^2 + \left(\frac{\sigma_{\rho_{\text{oil}}} + \sigma_{\rho_{\text{air}}}}{\rho_{\text{oil}} - \rho_{\text{air}}}\right)^2 + \left(\frac{\sigma_{V_{\text{stop}}}}{V_{\text{stop}}}\right)^2 \tag{20}$$

For Method 2:

$$\left(\frac{\sigma_{q_2}}{q_2}\right)^2 = (3\,\frac{\sigma_r}{r})^2 + \left(\frac{\sigma_d}{d}\right)^2 + \left(\frac{\sigma_g}{g}\right)^2 + \left(\frac{\sigma_{\rho_{\text{oil}}} + \sigma_{\rho_{\text{air}}}}{\rho_{\text{oil}} - \rho_{\text{air}}}\right)^2 + \left(\frac{\sigma_{V_{\text{rise}}}}{V_{\text{rise}}}\right)^2 + \left(\frac{\sigma_{v_d}}{v_d}\right)^2 + \left(\frac{\sigma_{v_u}}{v_u}\right)^2 \tag{21}$$

3.4 Final Charge

To test charge quantization, we analyzed the set of measured droplet charges $\{q_i\}$ by identifying integer multiplicities n_i such that $q_i \approx n_i e$. The smallest cluster of charges corresponded to $n = 1$, indicating that the greatest common divisor of all measured charges was consistent with one elementary charge. Using the lowest cluster (corresponding to singly charged droplets), we obtained an elementary charge of $e = (1.314 \pm 0.0126) \times 10^{-19}$C. Analysis of charges revealed that most droplets carried the single elementary charge (see Table 3). Charges corresponding to higher multiples were divided by their respective integer multiplicities n_i to obtain the equivalent single-charge values, from which the median was determined (see Table 3).

Table 5: Method-level charge estimates and quantization counts.

	Method 1 (Stopping)	**Method 2 (Rise & Fall)**
Mean $\bar{q}$ (C)	$(1.708 \pm 0.00927) \times 10^{-19}$	$(1.645 \pm 0.00884) \times 10^{-19}$
Median $\tilde{q}$ (C)	$(1.598 \pm 0.00826) \times 10^{-19}$	$(1.576 \pm 0.00814) \times 10^{-19}$
Multiplicity counts	$0e : 1,\ 1e : 83,\ 2e : 10$	$0e : 1,\ 1e : 86,\ 2e : 7$
Share of $1e$	88.3%	91.5%

4 Discussion

The analysis part suggests a median charge value of $(1.598 \pm 0.00826) \times 10^{-19}$ for method 1 and $(1.576 \pm 0.00814) \times 10^{-19}$ for method 2, which has a percent difference of 0.26% and 1.6% respect to the actual value of $e = 1.6022 \times 10^{-19}$C, showing a high accuracy. The analysis part also shows that around 90% of the droplets only contained one electron charge.

Although methods 1 and 2 calculated charges in totally different ways, where method 1 calculated charges with the stopping voltage, and method 2 calculated charges with the moving voltage, most of their results showed a similar value clustered around 1.6×10^{-19}C. However, the data from method 1 are more scattered, and it also seems to have a higher estimate compared to method 2, suggesting that there might be a larger uncertainty on V_{stop} or the voltages were incorrectly measured, especially since the droplets might be moving slowly rather than staying still.

4.1 Uncertainties

As the right apparatus worked much more efficiently than the other one, most data were measured with this apparatus, with a scale factor of 520 px/mm. However, a little data might be measured with the left apparatus, with a scale factor of 540 px/mm instead, which might cause an error in the analysis part. Meanwhile, both factors also have an error of ± 1 px/mm, and plus the inaccuracy of the Millikan experiment software when tracking the droplets, the speed measured thus has a non-negligible error, which would further affect the final value of charge q.

The distance between plates also has an unknown uncertainty. The data provided in the lab instruction only mentioned that $d = 6.0$mm, so we have to assume an uncertainty of ± 0.05mm according to the rule of rounding. Either the actual uncertainty is larger or smaller, the resulting uncertainty of q would be affected.

The instability of the applied voltage is another problem when collecting data. When we tried to obtain sufficient data on the movement of a droplet with a fixed voltage, it usually dropped by $0.5 - 2$V, causing a larger error in the end.

Other than the major causes mentioned above, some minor reasons may also affect the final result. Brownian motion introduces random fluctuations in a droplet's trajectory due to molecular collisions in air, which may blur position data and lead to scatter in the measured velocities. Moreover, non-uniform electric fields would be created if the plates are not perfectly parallel or if fringe effects near the chamber edges alter the field strength, letting droplets experience varying electric forces and biasing the calculated charge. Finally, droplet evaporation gradually reduces the droplet radius during observation, which causes slow drifts in the terminal velocity and apparent charge over time, and may also cause the Millikan software to lose tracking.

4.2 Potential Improvements

Although the lab itself measured the charge of an electron perfectly, a few problems appeared during the data collection steps, which directly prevented us from collecting enough data (at least 50 droplets) as a group.

The first serious problem that enormously delayed data collection is the usual tracking failure caused by the Millikan software. The failure usually happened under the following circumstances:

- 1 The droplet is moving fast
- 2 The droplet fades on screen
- 3 Other droplets are passing through the tracking box

As reason 2 might be an objective cause that cannot be solved, reasons 1 and 3 could be mitigated by introducing more advanced tracking algorithms or imaging (camera) with a higher frame rate. Implementing predictive tracking and background subtraction techniques would allow the software to maintain focus on a specific droplet even when it moves quickly or overlaps with others. These improvements would significantly enhance tracking stability, reduce data loss, and improve the accuracy of velocity and charge measurements.

Another issue encountered during the experiment was the instability of the applied voltage, which occasionally fluctuated even when the control setting was fixed. This fluctuation affected the balance of forces acting on the droplet and also made it difficult to measure the stopping or moving voltage accurately. Such variations introduced an enormous uncertainty into the calculation and further analysis. To improve measurement consistency, the voltage supply could be upgraded to a more stable regulated source, or the system could include a voltage monitoring circuit to continuously record the actual potential difference during data collection.

5 Conclusion

The experiment measured elementary charge as $e = 1.59 \pm 0.01 \times 10^{-19}$C, in excellent agreement with the $e = 1.6 \pm 0.01 \times 10^{-19}$C found in literature. The small deviation of the result (¡1%) confirms both accuracy and consistency of the two independent methods. Charge quantization was clearly observed as nearly all droplets carried integer multiples of the elementary charge, most just the elementary charge itself. Method 2 (rise & fall) showed slightly lower scatter than Method 1 (stopping). The dominant source of uncertainty was the radius term, voltage stability, plate spacing, and field uniformity. Despite these limitations, the results validated Millikan's findings and demonstrated the quantized nature of the electric charge.

References

[1] George E. Smith. *J. J. Thomson and The Electron: 1897–1899 — An Introduction*. Tech. rep. Published in The Chemical Educator. Provides historical context and analysis of Thomson's seminal papers on the electron. Department of Philosophy, Tufts University, 1997. URL: https://www.cs.princeton.edu/courses/archive/fall05/frs119/papers/smith97_thomson.pfg.pdf.

[2] Robert A. Millikan. "On the Elementary Electrical Charge and the Avogadro Constant". In: *Physical Review* 2 (1913), pp. 109–143. DOI: 10.1103/PhysRev.2.109. URL: https://doi.org/10.1103/PhysRev.2.109.

[3] C. Lee, N. Krasnopolskaia, et al. *The Millikan Oil-Drop Experiment*. March 17, 2025. Revisions by C. Lee (2023); N. Krasnopolskaia (2018); tk (1996); jbv (1994); gmg (1990). University of Toronto. 2025. URL: https://creativecommons.org/licenses/by-nc-sa/4.0/.

[4] Eivind Olav Dahl, Kjell-Eivind Frøysa, and Per Lunde. *Handbook of Uncertainty Calculations – Revision 2*. Revision 2, March 2003. Bergen and Oslo, Norway: Norwegian Society for Oil, Gas Measurement (NFOGM), and Norwegian Petroleum Directorate (NPD), 2003. ISBN: 82-91341-62-1. URL: https://nfogm.no/wp-content/uploads/2014/04/Handbook-of-uncertainty-calculations-r2-ISBN-82-91341-62-1.pdf.

[5] Michael Kearney. *Properties of Air: A Manual for Use in Biophysical Ecology (5th Edition)*. Accessed on 2025-10-28. NicheMapR Project. 2020. URL: https://mrke.github.io/NicheMapR/inst/doc/properties-of-air.

[6] National Institute of Standards and Technology. *Viscosity and Thermal Conductivity of Dry Air in the Gaseous Phase – Recommended Values*. Tech. rep. Uncertainties for the viscosities of gases are generally less than 3%. NIST, 2005. URL: https://tsapps.nist.gov/publication/get_pdf.cfm?pub_id=907539.

[7] Aleksandr Beliaev and Bob Dai. *Millikan Oil Drop Experiment Analysis Code*. https://github.com/alpha-trotsky/Milikan-Oil-Drop. GitHub repository, accessed October 28, 2025. 2025.